An Improved Metallicity Calibration with UBV Photometry

S. Karaali[A,C]*, S. Bilir*[B]*, S. Ak*[B]*, E. Yaz*[B]*, and B. Coşkunoğlu*[B]

[A] Beykent University, Faculty of Science and Letters, Department of Mathematics and Computer,
  Beykent Ayazağa Campus, 34398, Istanbul, Turkey
[B] Istanbul University, Faculty of Sciences, Department of Astronomy and Space Sciences,
  34119, Istanbul, Turkey
[C] Corresponding author. Email: karsa@istanbul.edu.tr

Abstract: We used the data of 701 stars covering the colour index interval $0.32 < B - V \leq 1.16$, with metallicities $-1.76 \leq$ [Fe/H] $\leq +0.40$ dex. The data were taken from the PASTEL catalogue and estimated metallicity-dependent guillotine factors, which provide a more accurate metallicity calibration. We reduced the metallicities of 11 different authors to the metallicities of Valenti & Fischer (2005), and thus obtained a homogeneous set of data which increased the accuracy of the calibration, i.e. [Fe/H] $= -14.316\delta_{0.6}^2 - 3.557\delta_{0.6} + 0.105$. Comparison of the metallicity residuals for two sets of data based on the metallicity-dependent guillotine factors with the ones obtained via metal-free guillotine factors shows that metallicities estimated by means of the new guillotine factors are more accurate than the other ones. This advantage can be used in the metallicity gradient investigation of the Galactic components, i.e. thin disc, thick disc, and halo.

**Keywords:** stars: abundances, stars: metallicity calibration, stars: metal poor

1 Introduction

Roman (1955) interpreted the weakness of the metallic lines in the F- and G-type spectra by comparison of the $B - V$ and $U - B$ colours for each star. She stated that an ultraviolet excess ranging from 0.0 to more than 0.2 mag, found in most high-velocity stars, is well correlated with the weakness of the lines. Moreover, both anomalies are correlated with velocity, in the sense that the stars with the weakest lines also have the largest ultraviolet excesses and the largest space velocities.

Following Schwarzschild et al. (1955), Sandage & Eggen (1959) interpreted the observed ultraviolet excess for subdwarfs with the 'blanketing model'. This model predicts that the change in $B - V$ colour index for a given observed ultraviolet excess, $\delta(U - B)$, for F and G subdwarfs is sufficient to move most of the subdwarfs with known M_V on the Hyades main sequence. The essential point of the theory is that the Fraunhofer lines affect the U, B, and V regions of the spectrum in different ways so that a weakening of the lines produces changes in the observed colour indices $U - B$ and $B - V$. If the relation between the effect on $U - B$ and $B - V$ is known, then the correction to the observed $B - V$ can be computed from the observed ultraviolet excess. Because the observed $B - V$ for weak-line stars will be bluer than that for strong-line stars of the same temperature, the weak-line stars will fall below the standard main sequence. Therefore, because of the relationship between $\Delta(U - B)$ and $\Delta(B - V)$ we should expect that the displacement of a weak-line star below the standard main sequence will be correlated with the observed ultraviolet excess. Wallerstein & Carlson (1960) calibrated the ultraviolet excess in terms of [Fe/H] for the first time, and Wallerstein (1962) improved this calibration. The scheme relating the observed ultraviolet excess $\delta(U - B)$ and the blanketing corrections $\Delta(U - B)$ and $\Delta(B - V)$ (for a hypothetical star) are given in Figure 1.

The shapes of the blanketing vectors in the $(U - B) - (B - V)$ diagram are such that stars with different $B - V$ values with the same metal abundances will show different values of ultraviolet excess. For red stars, $\delta(U - B)$ is partially guillotined because the blanketing line is nearly parallel to the intrinsic Hyades line. If the metal abundances are to be compared among stars of different colours, such as in the work carried out for the estimation of the metallicity gradient for the Galactic fields, corrections to the observed $\delta(U - B)$ are needed. Wildey et al. (1962) provided the basis on which normalized ultraviolet excess was computed by Sandage (1969) and Carney (1979). Sandage (1969) gave a procedure to correct guillotine effects on ultraviolet excess values for stars with the same metal abundances but different colours. He plotted 112 stars of large proper motion onto the $(U - B) - (B - V)$ two-colour diagram and compared the $U - B$ colours of maximum abundance with that of Hyades for the same $B - V$ colour. The results are given in Table 1. The columns give: (1) the $B - V$ colour; (2) the Hyades fiducial line; (3) the maximum $U - B$ value for the sample star for the same $B - V$ of the Hyades star; (4) the $\delta(U - B)$ ultraviolet excess of the sample star in
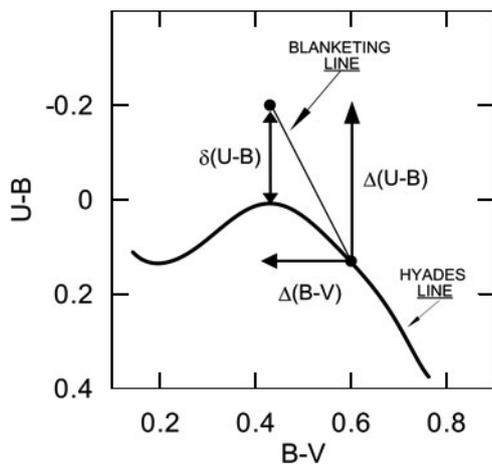
Figure 1 The scheme relating the observed ultraviolet excess, $\delta(U-B)$ and the blanketing corrections $\Delta(U-B)$ and $\Delta(B-V)$ taken from Sandage & Eggen (1959).

Table 1. The guillotine factors of Sandage (1969). $B-V$ indicates the $B-V$ colour, $(U-B)_H$ the Hyades fiducial line, $(U-B)_M$ the maximum $U-B$ value for the sample star for the same $B-V$ of the Hyades star, $\delta(U-B)$ the $\delta(U-B)$ ultraviolet excess of the sample star in question, and $\delta_{0.6}/\delta(U-B)$ the ratio of the excess at $(B-V) = 0.60$ (where $\delta(U-B)$ is maximum), $\delta_{0.6}$, to the excess at any other $B-V$

$B-V$	$(U-B)_H$	$(U-B)_M$	$\delta(U-B)$	$\delta_{0.6}/\delta(U-B)$
0.35	0.03	−0.22	0.25	1.24
0.40	0.01	−0.25	0.26	1.19
0.45	0.00	−0.27	0.27	1.15
0.50	0.03	−0.25	0.28	1.11
0.55	0.08	−0.22	0.3	1.03
0.60	0.13	−0.18	0.31	1
0.65	0.19	−0.11	0.3	1.03
0.70	0.25	−0.03	0.28	1.1
0.75	0.34	0.08	0.26	1.19
0.80	0.43	0.19	0.24	1.29
0.85	0.54	0.32	0.22	1.41
0.90	0.64	0.44	0.2	1.55
0.95	0.74	0.55	0.19	1.63
1.00	0.84	0.67	0.17	1.82
1.05	0.94	0.79	0.15	2.06
1.10	0.99	0.87	0.12	2.58

question; and (5) the ratio of the excess at $(B-V) = 0.60$ (where $\delta(U-B)$ is maximum), $\delta_{0.6}$, to the excess at any other $B-V$. This ratio is defined as the 'guillotine factor' in this paper, i.e. $f_S = \delta_{0.6}/\delta(U-B)$, where the subscript S refers to Sandage. Table 1 gives the guillotine factors of Sandage (1969) for a set of 16 colours with $0.35 \leq B-V \leq 1.10$. One can estimate guillotine factors for a larger set of $B-V$ colours by applying an interpolation formula to the data in Table 1. This is the case in some of our works (Karaali et al. 2003; Ak et al. 2007a, 2007b; Yaz & Karaali 2010).

Carney (1979) normalized the ultraviolet excesses of 101 dwarfs by using the procedure of Sandage (1969) and calibrated them to the metal abundance [Fe/H]. This calibration could be used to evaluate metal abundances in the UBV photometry. Karaali et al. (2003) improved this calibration by using a different procedure and a different set of UBV data. Other works in different photometries followed the ones carried out in the UBV for metallicity estimation. Buser & Fenkart (1990) calibrated the [Fe/H] metal abundance to the normalized $\delta(U-G)$ excess and $(G-R)$ colour, simultaneously, in the RGU photometry. Strömgren (1966) defined the $m_1 = (v-b) - (b-y)$ colour difference as a metallicity indicator, where v, b, and y are magnitudes for intermediate bands in his $uvby - \beta$ photometry and the $(B-L)$ colour turned out to be a very sensitive metallicity index for F–G spectral type stars in the $VBLUW$ photometry (Walraven & Walraven 1960; Trefzger et al. 1995).

There are deviations between the calibrations obtained for the UBV system. Figure 15 of Buser & Kurucz (1992) compares these calibrations based on empirical data (Carney 1979; Cameron 1985) or theoretical models (Buser & Kurucz 1978, 1985; Vandenberg & Bell 1985). The reason for these differences originates from two sources. Firstly, although researchers use the UBV data of the same stars, the references and hence the UBV magnitudes or colours therein may be different. Secondly, different atmospheric parameters may be used by different researchers in estimation of the metallicities used for [Fe/H]-$\delta_{0.6}$ calibration (cf. Cayrel de Strobel et al. 2001).

The guillotine factors of Sandage (1969) are colour dependent, but not metallicity dependent. However, the isometallicity lines in the $(U-B)-(B-V)$ two-colour diagram are not parallel to each other for the whole colour range of $B-V$, which indicates the dependence of the guillotine factors on the metallicity. This is the main topic of the paper. The data are presented in Section 2. The guillotine factors and the metallicity calibration are given in Section 3, and finally a short discussion is presented in Section 4.

2 The Data

The PASTEL catalogue (Soubiran et al. 2010) is the main source of data for our study. 4259 stars with $4 \leq \log g \leq 5$ and with known metallicity and metallicity errors were selected as main sequence stars from the PASTEL catalogue. 3187 of these stars, that were not displaying variability in their magnitudes and were tagged as 'star', 'star in cluster', and 'high proper motion star' in SIMBAD, were used in the study. To obtain UBV data, we consulted the specialized catalogues which are included in the General Catalogue of Photometric Data (Hauck et al. 1990), which provided the data for 2073 stars.

To calibrate the metallicity more accurately, we selected 11 authors appearing in the PASTEL catalogue (Soubiran et al. 2010), whose databases coincide the most with the 2073 stars in our study. These authors are: Valenti & Fischer (2005), Sousa et al. (2008), Ramirez & Melendez (2005), Santos et al. (2004), Fuhrmann (2008), Luck & Heiter (2006), Mishenina et al. (2004), Nissen

et al. (2002), Ryan & Smith (2003), Spite et al. (1996), and Tomkin & Lambert (1999). From all authors we collected a total of 701 stars, the metal abundances of 472 of which were determined by Valenti & Fischer (2005). Hence, we reduced all the metallicities to Valenti & Fischer (2005)'s using the calibrations between the metal abundances of common stars in the work of Valenti & Fischer (2005) and other researchers. Table 2 gives the star catalogue obtained by this procedure. The errors cited for the metal abundances belong to the original figures. The parallaxes were taken from the newly reduced Hipparcos catalogue (van Leeuwen 2007). The $U BV$ data of stars in Table 2 have been dereddened by the following procedure (Bahcall & Soneira 1980).

$$A_d(b) = A_\infty(b) \times \left(1 - e^{\frac{-|d \sin(b)|}{H}}\right) \qquad (1)$$

where b and d are the Galactic latitude and the distance of the star (evaluated by means of its parallax), respectively. H is the scale height for the interstellar dust, which is adopted as 125 pc (Marshall et al. 2006), and $A_\infty(b)$ and $A_d(b)$ are the total absorptions for the model (Schlegel et al. 1998) and for the distance to the star respectively. $A_\infty(b)$ may be evaluated by means of Equation 2.

$$A_\infty(b) = 3.1 \times E_\infty(B - V), \qquad (2)$$

where $E_\infty(B - V)$ is the colour excess for the model taken from the NASA Extragalactic Database.[1] Then, $E_d(B - V)$, i.e. the colour excess for the corresponding star at the distance d, can be evaluated by Equation 2 adapted for distance d,

$$E_d(B - V) = A_d(b)/3.1, \qquad (3)$$

and can be used for the colour excess $E_d(U - B)$ evaluation:

$$E_d(U - B) = 0.72 E_d(B - V) + 0.05 E_d^2(B - V). \quad (4)$$

Finally, the dereddened colour indices are:

$$(B - V)_0 = (B - V) - E_d(B - V)$$
$$(U - B)_0 = (U - B) - E_d(U - B). \qquad (5)$$

The reduced ultraviolet excess $\delta_{0.6}$ is evaluated by the following equation which is obtained from the data of 133 stars with $0.575 \le (B - V) \le 0.625$ (Table 3):

$$\delta_{0.6} = -0.038(0.005)[Fe/H]^3 - 0.163(0.019)[Fe/H]^2$$
$$- 0.302(0.017)[Fe/H] + 0.012(0.004). \qquad (6)$$

In this study, Karaali's guillotine factor is denoted by f_K and is calculated with $f_K = \delta_{0.6}/\delta$.
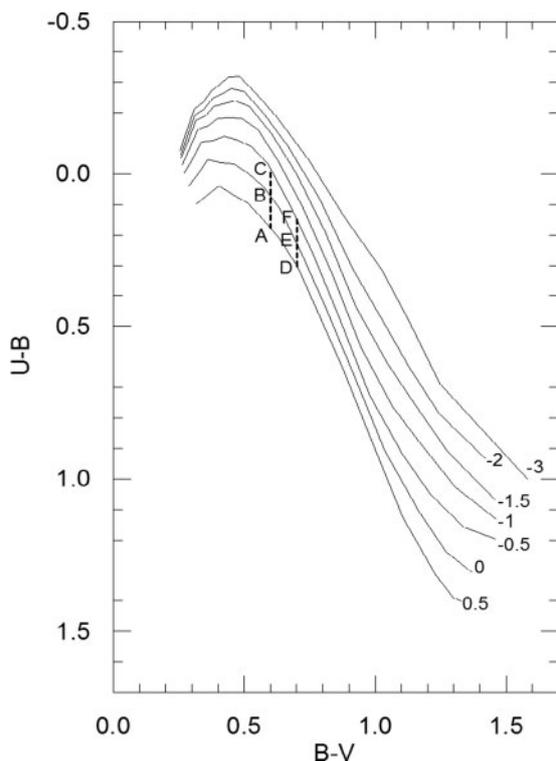
Table 2. Data used for metallicity calibration. The columns show: CD, BD, HD, or G (Giclas) number, (α, δ) and (l, b) equatorial and Galactic coordinates, distance (pc), dereddened $U BV$ data, reduced ultraviolet excess $\delta_{0.6}$, original metallicity [Fe/H] and its error, metallicity reduced to Valenti & Fischer (2005) system [Fe/H]$_{VF}$ and the author. The coordinates are defined as in ICRS

Star	α	δ	l	b	d	V_0	$(B - V)_0$	$(U - B)_0$	$\delta_{0.6}$	[Fe/H]	[Fe/H]$_{err}$	[Fe/H]$_{VF}$	Author
HD000055	00 05 17.670	−67 49 57.73	309.497	−48.703	16	8.486	1.062	0.863	0.15	−0.66	0.02	−0.64	Sousa
HD000101	00 05 54.739	+18 14 05.83	108.005	−43.313	37	7.431	0.554	0.036	0.08	−0.28	0.04	−0.25	Ramirez
HD000142	00 06 19.215	−49 04 30.76	321.587	−66.387	26	5.694	0.514	0.021	−0.03	0.10	0.03	0.14	Valenti
HD000283	00 07 32.507	−23 49 07.50	48.982	−79.560	33	8.675	0.795	0.336	0.13	−0.55	0.03	−0.52	Valenti
HD000400	00 08 40.373	+36 37 37.76	113.443	−25.426	32	6.155	0.486	−0.070	0.06	−0.21	0.03	−0.18	Valenti
⋮	⋮	⋮	⋮	⋮	⋮	⋮	⋮	⋮	⋮	⋮	⋮	⋮	⋮
HD223498	23 50 05.768	+02 52 38.04	94.302	−56.546	45	8.305	0.733	0.354	−0.08	0.23	0.03	0.27	Valenti
HD224022	23 54 38.598	−40 18 00.16	341.042	−72.356	28	6.013	0.572	0.106	−0.05	0.15	0.06	0.19	Sousa
HD224156	23 55 32.411	+03 30 04.95	97.015	−56.531	30	7.685	0.746	0.346	0.01	−0.03	0.03	0.00	Valenti
HD224383	23 57 33.478	−09 38 50.59	84.366	−68.386	48	7.826	0.629	0.137	0.02	−0.04	0.03	−0.01	Valenti
HD224619	23 59 28.388	−20 02 05.06	60.981	−76.155	25	7.456	0.740	0.281	0.06	−0.20	0.01	−0.17	Sousa

Table 3. Stars with $0.575 \leq B - V \leq 0.625$ used for calibration of $\delta_{0.6}$ to metallicity. The columns show: CD, BD, HD, or G (Giclas) number, dereddened UBV data, metallicity reduced to Valenti & Fischer (2005) and reduced ultraviolet excess $\delta_{0.6}$

Star	$(B-V)_o$	$(U-B)_o$	[Fe/H]	$\delta_{(0.6)}$
HD020407	0.576	−0.023	−0.42	0.128
HD043745	0.577	0.078	0.13	0.028
HD003149	0.578	0.061	−0.07	0.046
HD134088	0.578	−0.059	−0.75	0.166
HD104800	0.578	−0.059	−0.82	0.166
HD145809	0.578	0.057	−0.24	0.05
HD188510	0.578	−0.131	−1.64	0.238
BD+660268	0.580	−0.147	−2.09	0.257
HD286891	0.580	−0.040	−0.56	0.15
HD030649	0.580	0.029	−0.49	0.081
HD078366	0.580	0.039	0.08	0.071
HD126681	0.581	−0.115	−1.16	0.226
HD029461	0.581	0.145	0.25	−0.034
HD006500	0.582	−0.009	−0.60	0.121
HD007983	0.582	−0.028	−0.60	0.14
HD115383	0.582	0.093	0.28	0.019
HD196850	0.582	0.071	−0.11	0.041
HD199288	0.582	−0.045	−0.63	0.157
HD165499	0.583	0.055	0.01	0.058
HD044120	0.583	0.080	0.10	0.033
HD133161	0.583	0.165	0.21	−0.052
HD158226	0.584	−0.028	−0.52	0.142
BD+592407	0.584	−0.103	−1.95	0.217
HD171990	0.585	0.114	0.07	0.001
HD083529	0.585	0.019	−0.25	0.096
HD206332	0.585	0.169	0.27	−0.054
HD059360	0.586	0.087	−0.12	0.029
HD129290	0.586	0.062	−0.13	0.054
HD018709	0.586	−0.003	−0.26	0.119
HD131117	0.586	0.087	0.14	0.029
HD170778	0.586	0.087	0.00	0.029
HD014056	0.587	−0.012	−0.61	0.129
HD111367	0.587	0.086	−0.18	0.031
G 232−18	0.587	−0.019	−0.80	0.136
HD124553	0.587	0.143	0.28	−0.026
HD093745	0.587	0.111	0.08	0.006
HD041330	0.588	0.051	−0.14	0.067
HD019373	0.588	0.113	0.16	0.005
HD052711	0.588	0.058	−0.10	0.06
HD168871	0.588	0.046	−0.09	0.072
HD088742	0.589	0.073	−0.05	0.046
HD283807	0.590	0.000	−0.58	0.12
HD121004	0.591	−0.056	−0.80	0.177
HD001388	0.591	0.088	0.00	0.033
HD016623	0.591	0.007	−0.45	0.114

Star	$(B-V)_o$	$(U-B)_o$	[Fe/H]	$\delta_{(0.6)}$
HD155918	0.592	−0.017	−0.64	0.139
HD024040	0.593	0.198	0.21	−0.074
HD039091	0.593	0.094	0.05	0.03
HD102158	0.593	0.038	−0.47	0.086
HD196800	0.593	0.137	0.16	−0.013
HD221830	0.593	0.057	−0.40	0.067
HD061383	0.594	0.024	−0.48	0.101
BD+730943	0.594	0.016	−0.37	0.109
HD070110	0.594	0.142	0.15	−0.017
HD088986	0.594	0.156	0.09	−0.031
HD096700	0.594	0.065	−0.18	0.06
HD009782	0.595	0.086	0.09	0.04
HD009782	0.595	0.086	0.15	0.04
HD045391	0.595	0.016	−0.50	0.11
HD073524	0.595	0.116	0.12	0.01
HD067458	0.596	0.036	−0.19	0.091
HD110898	0.597	0.009	−0.38	0.119
HD004307	0.597	0.069	−0.19	0.059
HD020807	0.598	0.001	−0.26	0.128
HD143761	0.598	0.083	−0.20	0.046
HD150433	0.599	0.047	−0.38	0.083
HD070923	0.600	0.097	0.12	0.034
HIP043595	0.600	−0.040	−0.80	0.171
HD006434	0.600	−0.012	−0.52	0.143
HD150706	0.600	0.076	−0.01	0.055
HD088218	0.600	0.148	−0.14	−0.017
HD088725	0.600	−0.016	−0.70	0.147
HD107146	0.600	0.071	−0.03	0.06
HD090508	0.601	0.054	−0.30	0.078
HD165401	0.601	0.021	−0.36	0.111
HD222033	0.601	0.121	0.19	0.011
HD010226	0.602	0.134	0.22	0
HD211415	0.603	0.059	−0.20	0.076
HD218209	0.604	0.049	−0.46	0.087
HD056274	0.605	−0.018	−0.55	0.155
HD073668	0.605	0.079	0.00	0.058
HD095128	0.605	0.123	0.04	0.014
HD164427	0.605	0.117	0.13	0.02
HD197076	0.607	0.071	−0.09	0.068
HD009224	0.608	0.108	0.00	0.032
HD149612	0.608	0.024	−0.45	0.116
HD114729	0.609	0.044	−0.26	0.097
HD118475	0.609	0.166	0.10	−0.025
HD223238	0.609	0.128	0.02	0.013
HD134060	0.610	0.139	0.09	0.003

Star	$(B-V)_o$	$(U-B)_o$	[Fe/H]	$\delta_{(0.6)}$
HD221146	0.611	0.214	0.11	−0.070
HD010519	0.612	0.027	−0.58	0.118
HD013043	0.612	0.145	0.09	0.000
HD033021	0.612	0.080	−0.14	0.065
HD084737	0.612	0.143	0.17	0.002
HD054351	0.613	0.115	−0.05	0.031
HD064090	0.614	−0.129	−1.80	0.276
HD030562	0.614	0.181	0.26	−0.034
HD068978	0.614	0.067	0.02	0.080
HD139324	0.614	0.156	0.15	−0.009
HD094835	0.615	0.116	0.13	0.032
HD178496	0.615	0.119	−0.26	0.029
HD120066	0.615	0.147	0.11	0.001
HD166435	0.615	0.086	0.04	0.062
BD+591609	0.616	0.070	−0.45	0.079
HD003074	0.616	0.146	0.00	0.003
HD066171	0.616	0.057	−0.31	0.092
HD208704	0.617	0.109	−0.08	0.041
HD152792	0.617	0.091	−0.31	0.059
HD250792	0.618	−0.043	−1.07	0.195
HD001832	0.618	0.121	−0.03	0.031
HD008262	0.618	0.091	−0.16	0.061
HD051419	0.618	0.069	−0.40	0.083
HD053705	0.618	0.045	−0.21	0.107
HD097998	0.619	0.052	−0.41	0.101
HD216435	0.619	0.169	0.24	−0.016
HD036283	0.620	0.083	−0.31	0.071
HD031966	0.621	0.215	0.13	−0.060
HD038858	0.621	0.086	−0.23	0.069
HD034411	0.622	0.121	0.12	0.035
HD071148	0.622	0.118	0.02	0.038
HD071881	0.622	0.134	−0.05	0.022
HD183658	0.623	0.158	0.05	−0.001
HD042618	0.624	0.119	−0.11	0.040
HD088371	0.624	0.109	−0.31	0.050
HD199960	0.624	0.213	0.27	−0.054
HD018757	0.625	0.128	−0.28	0.032
CD−2808426	0.625	0.019	−0.64	0.141
HD147231	0.625	0.216	0.00	−0.056
HD179140	0.625	0.162	0.12	−0.002
HD196068	0.625	0.273	0.31	−0.113
HD200565	0.625	0.112	−0.06	0.048
BD+38 4955	0.660	−0.160	−2.50	0.340

Figure 2 Synthetic isometallicity lines for UBV photometry taken from a stellar model of Lejeune et al. (1997).
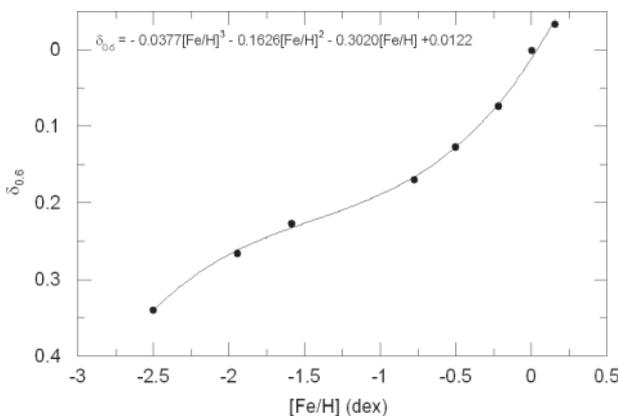
Figure 3 Metallicity versus ultraviolet excess calibration for 133 stars with $0.575 \leq B - V \leq 0.625$.

3 Methods

3.1 New Guillotine Factors

Sandage (1969) estimated guillotine factors without considering the effect of metallicity. However, Figure 2 shows that the colour gradients for any two different isometallicity lines are not equal to each other, i.e. $\frac{|AB|}{|DE|} \neq \frac{|AC|}{|DF|}$, which indicates the dependence of guillotine factors on metallicity. Additionally, the $(U - B)_M$ colours in Table 1 correspond to the stars with less metallicity than the Hyades cluster. But the metallicity gradients for the isometallicity line with [Fe/H] = 0.5 dex in Figure 2 are rather different from the ones for relatively metal-poor

stars, which indicates that guillotine factors for metal-rich stars should be different from those of metal-poor stars of the same $B - V$ colour index.

Then we decided that it should be more appropriate and useful to estimate metallicity-dependent guillotine factors. First, we used 133 stars with colour index $0.575 \leq B - V \leq 0.625$ and calibrated their ultraviolet excess to the metallicity. The calibration (Equation 6) provides ultraviolet excess reduced to $B - V = 0.60$ for any star with metal abundance [Fe/H] ≥ -2.5 dex. Thus, we can use the calibration obtained from Figure 3 to estimate reduced $\delta_{0.6}$ ultraviolet excess for stars with metal abundance $-2.5 \leq$ [Fe/H] ≤ 0.15 dex.

Next, we separated the stars in Table 2 into eight subsamples with colour indices $0.32 < B - V \leq 0.42$, $0.42 < B - V \leq 0.49$, $0.49 < B - V \leq 0.57$, $0.57 < B - V \leq 0.62$, $0.62 < B - V \leq 0.69$, $0.69 < B - V \leq 0.76$, $0.76 < B - V \leq 0.85$, $0.85 < B - V \leq 1.16$ and obtained calibrations for the guillotine factors as follows. The number of these colour intervals and their ranges had been decided so as to obtain a constant metallicity gradient for each $B - V$ interval. For example, the ranges for bluer stars, where the metallicity gradient is relatively large, were chosen to be smaller than for the colour interval $0.85 < B - V \leq 1.16$, where the metallicity gradient is relatively small. The $(U - B) - (B - V)$ colour diagrams of the whole sample and eight subsamples are shown in Figure 4.

Each subsample was divided into bins and mean δ, $B - V$, $U - B$, [Fe/H], $(U - B)_H$, $\delta_{0.6}$, and f_K values were evaluated for each subsample (Table 4). A total of 532 stars could be used in the calibration of guillotine factors. The ultraviolet excess δ of a sample star whose $U - B$ colour index is close to that of a Hyades star of the same $B - V$ colour index is rather small. Hence $f_K = \delta_{0.6}/\delta$ becomes rather large for such stars, and they are not reliable. These abnormal f_K values may be as large as 20, for example. Also, we noted that the f_K values of some stars were negative. The reason for these unreliable values is errors in the $U - B$ colour index. After rejecting the stars with large and negative f_K values, the number of stars was reduced from 701 to 532. The number of stars used in each bin is given in the last column of Table 4.

The calibration of δ to f_K is given in Figure 5. It is noticeable that the relation of δ to f_K is smooth in all panels, and that the trend of the guillotine factor varies in different panels. In panels (a), (b), (g), and (h), f_K assumes its maximum value at intermediate values of δ, whereas in panels (c), (d), (e), and (f) the maximum of f_K corresponds to negative values of δ, i.e. metal-rich stars. Figure 6 shows the calibration of $B - V$ to f_K for three ultraviolet excesses, $\delta = -0.05$, $+0.05$, and $+0.15$, just to show that one can obtain continuous transitions between colour index and ultraviolet excess. Since Figure 5 is divided according to colours and the fits are in better agreement with data, the obtained equations will be more precise. Therefore, we prefer the equations obtained from Figure 5.
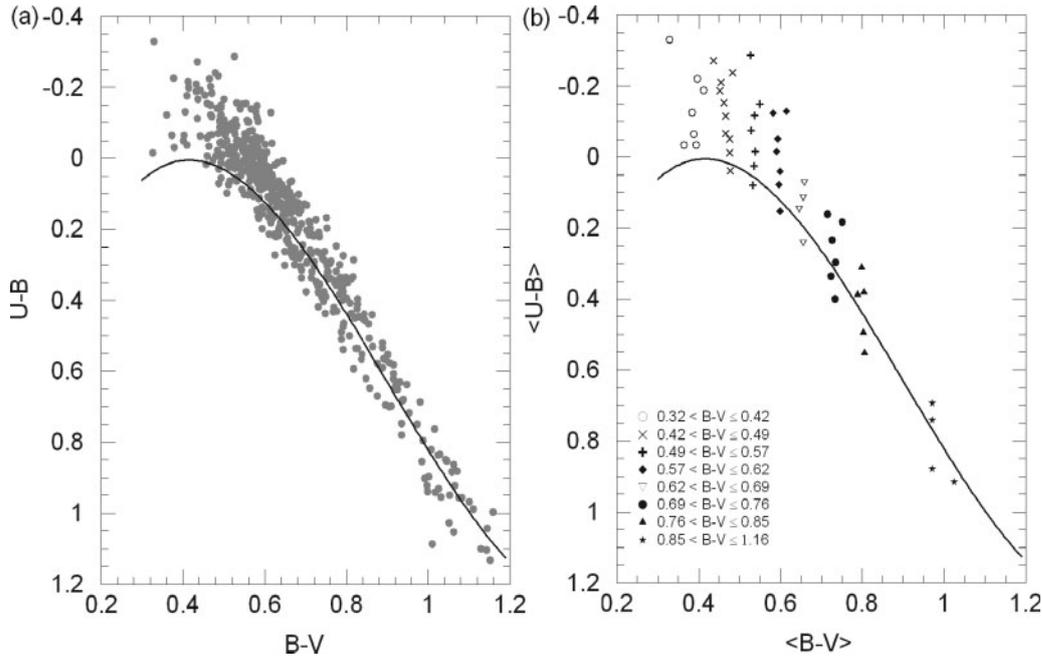
Figure 4 $(U-B)-(B-V)$ two-colour diagrams for (a) the whole sample, and (b) 50 bins of eight subsamples in Table 4.

Figure 7 shows the distribution of the guillotine factors as a function of metallicity. The lower limit for the guillotine factors of Sandage (1969) is $f_S = 1$ (Figure 7(b)), corresponding to the colour index $B - V = 0.60$, whereas the one estimated in this work may be less than 0.5, which is not colour dependent, but corresponds to metal abundance $[Fe/H] \approx 0$ dex.

3.2 New Metallicity Calibration

We used the calibrations in Figure 5 and assigned guillotine factors, f_K, for 701 stars with metallicity $-1.76 \leq [Fe/H] \leq +0.40$ dex. The combination of f_K and the ultraviolet excess δ gives the reduced ultraviolet excess for each star, i.e. $\delta_{0.6} = f_K \times \delta$. Then we divided the interval $-0.15 \leq \delta_{0.6} \leq 0.24$ into 11 scans and adopted the centroid of each scan as a locus point to fit a second-order polynomial (Figure 8) to the points ($\delta_{0.6}$, $[Fe/H]$). The full equation of the polynomial is

$$[Fe/H] = -14.316(1.919)\delta_{0.6}^2 + 3.557(0.285)\delta_{0.6} + 0.105(0.039). \tag{7}$$

Equation 7 provides metallicities by means of new guillotine factors. We used the guillotine factors of Sandage (1969) and evaluated another set of reduced $\delta_{0.6}$ ultraviolet excesses for the same star sample. Their fit to the corresponding metallicities is given in Figure 8 and in the following formula:

$$[Fe/H] = -11.612(0.496)\delta_{0.6}^2 + 3.419(0.100)\delta_{0.6} + 0.057(0.017). \tag{8}$$

3.3 Application of the Method

Now, we have two metallicity calibrations, based on the new guillotine factors estimated in this work and on the guillotine factors adopted from Sandage (1969). We applied these calibrations to two sets of data with $-1.76 \leq [Fe/H] \leq 0.4$ dex taken from Karaali et al. (2003) and Karataş & Schuster (2006) and we compared the evaluated metallicities with the original ones for two calibrations. The metallicities of 75 stars in the first set were estimated spectroscopically, whereas those for 469 stars are based on photometry. There is no overlap between stars in the two sets just mentioned and the sample stars. The results for the data of Karaali et al. (2003) are given in Table 5. The column headings are as follows: Hip No is the Hipparcos number; δ is the ultraviolet excess; f_K and f_S are the guillotine factors estimated in this work and adopted from Sandage (1969), respectively; $\delta_{0.6}(K)$ and $\delta_{0.6}(S)$ are ultraviolet excesses reduced by means of f_K and f_S, respectively; $[Fe/H]_{obs}$, $[Fe/H]_K$, and $[Fe/H]_S$ are original metallicities taken from the literature and metallicities evaluated via Equations 7 and 8, respectively; $\Delta[Fe/H]_K$ and $\Delta[Fe/H]_S$ are residuals for two calibrations, where K and S refer to the data evaluated by means of the guillotine factors estimated in this work and those adopted from Sandage (1969). The results for all 469 stars are not given here in order to save space. However, their statistics are given in Table 6 together with those of 75 stars in the first set.

Comparison of the mean and standard deviations for the residuals of two calibrations for four metallicity intervals, i.e. $-1.76 [Fe/H] \leq -1$, $-1 < [Fe/H] \leq -0.5$, $-0.5 < [Fe/H] \leq 0$, and $0 < [Fe/H] \leq +0.4$ dex shows

Table 4. Ultraviolet excess δ, reduced ultraviolet excess $\delta_{0.6}$ and new guillotine factors f_K for each bin of eight sub-samples. $\langle B - V \rangle$ and $\langle U - B \rangle$ are the mean colours, $\langle [\text{Fe/H}] \rangle$ is the mean metallicity, $\langle (U - B)_{\text{H}} \rangle$ is the mean Hyades sequence, and N is the number of stars in each bin

| $\langle B - V \rangle$	$\langle U - B \rangle$	$\langle [\text{Fe/H}] \rangle$	$\langle (U - B)_{\text{H}} \rangle$	δ	$\delta_{0.6}$	f_K	N
$0.32 < B - V \leq 0.42$							
0.394	−0.034	−0.053	0.012	0.046	0.028	0.595	2
0.364	−0.033	−0.110	0.031	0.064	0.043	0.695	2
0.388	−0.064	−0.224	0.014	0.079	0.071	0.924	2
0.384	−0.126	−0.584	0.017	0.143	0.140	0.985	2
0.412	−0.188	−1.424	0.008	0.195	0.221	1.135	2
0.396	−0.220	−1.836	0.012	0.233	0.254	1.092	2
0.329	−0.330	−1.530	0.050	0.379	0.229	0.603	1
$0.42 < B - V \leq 0.49$							
0.477	0.039	0.082	0.018	−0.021	−0.014	0.819	3
0.475	−0.012	−0.054	0.017	0.029	0.027	0.964	6
0.475	−0.051	−0.228	0.017	0.068	0.073	1.082	2
0.466	−0.066	−0.307	0.014	0.08	0.090	1.152	4
0.466	−0.115	−0.633	0.014	0.129	0.145	1.119	4
0.462	−0.153	−0.981	0.013	0.166	0.187	1.128	4
0.452	−0.186	−1.268	0.01	0.196	0.210	1.072	6
0.455	−0.211	−1.443	0.011	0.222	0.223	1.003	3
0.482	−0.237	−1.763	0.019	0.256	0.249	0.973	2
0.436	−0.271	−1.745	0.007	0.278	0.244	0.879	1
$0.49 < B - V \leq 0.57$							
0.532	0.080	0.188	0.052	−0.028	−0.053	1.787	12
0.535	0.026	−0.085	0.054	0.028	0.036	1.273	24
0.537	−0.016	−0.307	0.056	0.072	0.087	1.209	38
0.528	−0.075	−0.641	0.049	0.124	0.146	1.182	27
0.536	−0.117	−1.069	0.056	0.173	0.194	1.127	10
0.549	−0.150	−1.414	0.065	0.216	0.217	1.006	4
0.526	−0.286	−1.211	0.046	0.332	0.206	0.623	1
$0.57 < B - V \leq 0.62$							
0.598	0.153	0.161	0.116	−0.037	−0.042	1.387	19
0.595	0.078	−0.096	0.113	0.035	0.039	1.098	23
0.598	0.041	−0.321	0.117	0.076	0.089	1.195	29
0.590	−0.015	−0.546	0.107	0.121	0.133	1.097	21
0.593	−0.051	−0.85	0.111	0.162	0.174	1.073	5
0.581	−0.124	−1.71	0.096	0.22	0.245	1.112	4
0.614	−0.129	−1.801	0.136	0.265	0.249	0.941	1
$0.62 < B - V \leq 0.69$							
0.655	0.243	0.201	0.192	−0.05	−0.057	1.274	34
0.645	0.147	−0.111	0.179	0.032	0.042	1.288	22
0.655	0.115	−0.276	0.193	0.078	0.081	1.038	29
0.658	0.073	−0.611	0.196	0.123	0.143	1.177	12
$0.69 < B - V \leq 0.76$							
0.732	0.401	0.387	0.317	−0.084	−0.133	1.611	6
0.722	0.335	0.218	0.3	−0.035	−0.064	1.650	13
0.734	0.296	−0.098	0.321	0.025	0.038	1.555	11
0.726	0.234	−0.429	0.306	0.073	0.109	1.525	17
0.714	0.161	−0.604	0.286	0.125	0.141	1.143	4
0.751	0.183	−0.886	0.351	0.168	0.164	0.955	2
$0.76 < B - V \leq 0.85$							
0.806	0.550	0.328	0.454	−0.096	−0.106	1.127	5
0.803	0.491	0.22	0.447	−0.044	−0.063	1.461	10
0.789	0.385	−0.175	0.422	0.036	0.060	1.737	11
0.805	0.378	−0.458	0.453	0.075	0.117	1.614	17
0.799	0.308	−0.583	0.44	0.132	0.134	1.024	8
$0.85 < B - V \leq 1.16$							
0.972	0.878	0.36	0.782	−0.097	−0.121	1.332	11
1.025	0.915	0.215	0.877	−0.038	−0.062	1.627	11
0.971	0.741	−0.165	0.776	0.035	0.055	1.539	21
0.971	0.693	−0.373	0.777	0.083	0.100	1.214	22
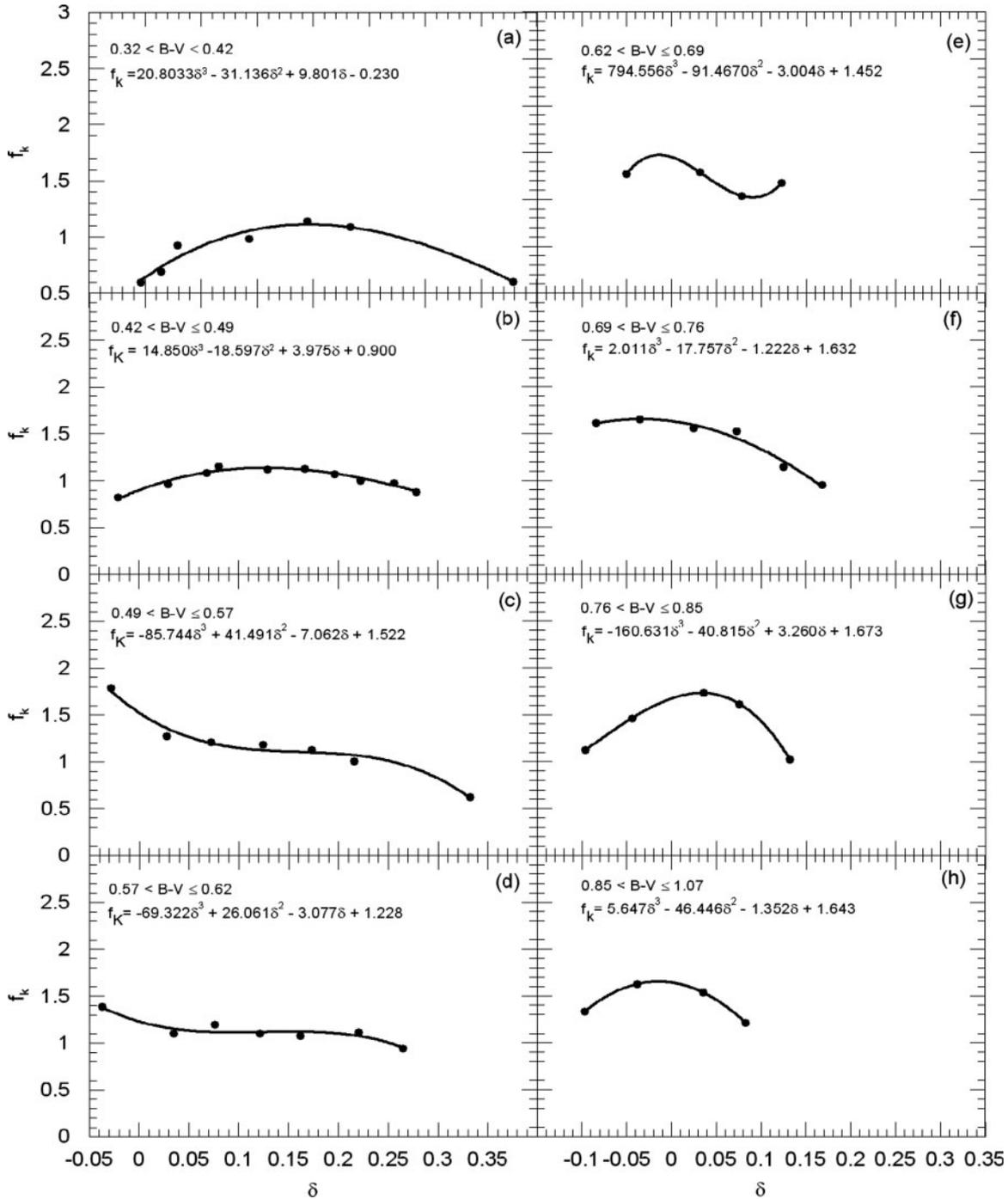
Figure 5   Calibration of ultraviolet excess (δ) to the guillotine factor f_K for eight subsamples.

that there are statistical differences between the two calibrations. In Table 6(a), where the statistics for the first set (75 stars) are presented, the agreement is only for the interval $-1 < [Fe/H] \leq -0.5$ dex, whereas for other metallicity intervals, the calibration based on metallicity-dependent guillotine factors f_K is favored. The largest differences between the two sets of statistics occur among the metal-poor stars, i.e. $-1.76 < [Fe/H] \leq -1$ dex. In Table 6(b), where the statistics correspond to a larger set of data (469 stars) and where the metallicities were determined photometrically, the agreement between

the two calibrations is only for the metallicity interval $-1.76 < [Fe/H] \leq -1$ dex. The mean deviation of the residuals estimated via guillotine factors f_S for the metallicity interval $-0.5 < [Fe/H] \leq 0$ dex is a bit smaller than the ones estimated via f_K (0.01 and -0.03 respectively), whereas for the two metallicity intervals $-1 < [Fe/H] \leq -0.5$ and $0 < [Fe/H] \leq +0.4$ dex the mean deviations corresponding to f_K are much smaller than those of f_S.

The comparison of the residuals for all metallicities, i.e. $-1.76 < [Fe/H] \leq +0.4$ dex, estimated by means of the two calibrations (Figures 9 and 10) confirms the advantage
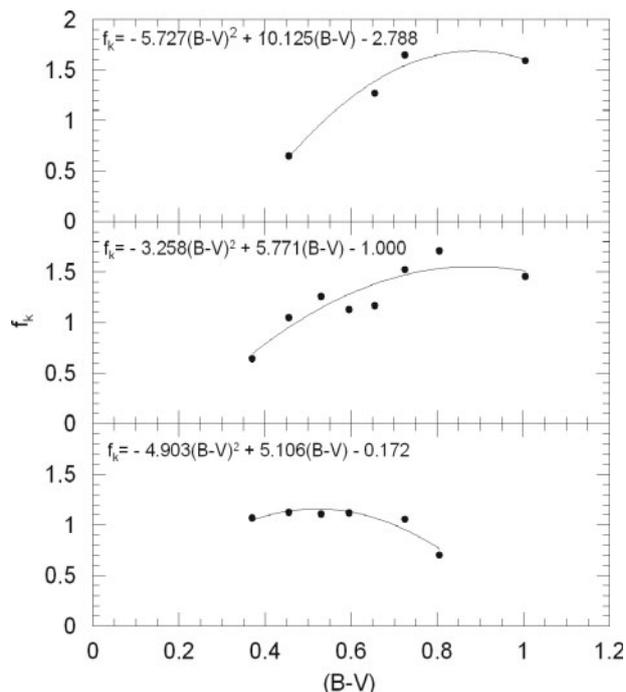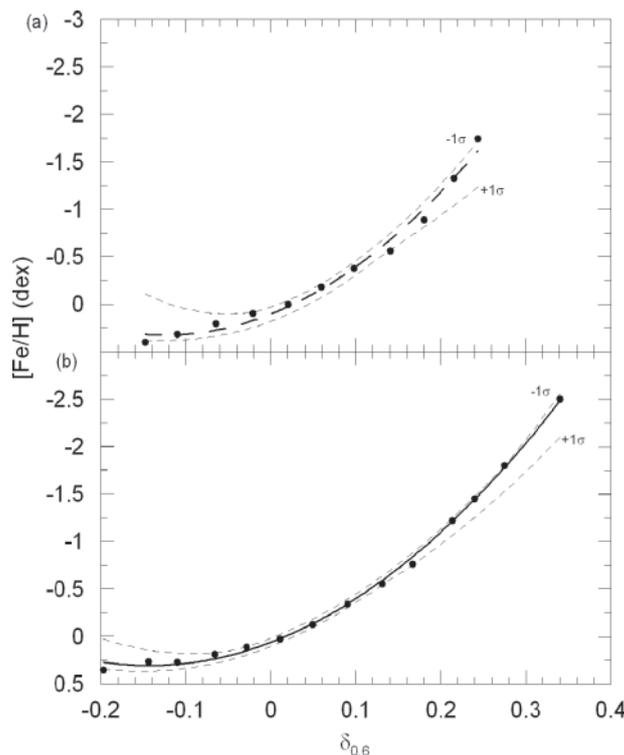
Figure 6 Calibration of $B - V$ colour to the guillotine factor f_K for three ultraviolet excesses, $\delta = -0.05$, $+0.05$, and $+0.15$.
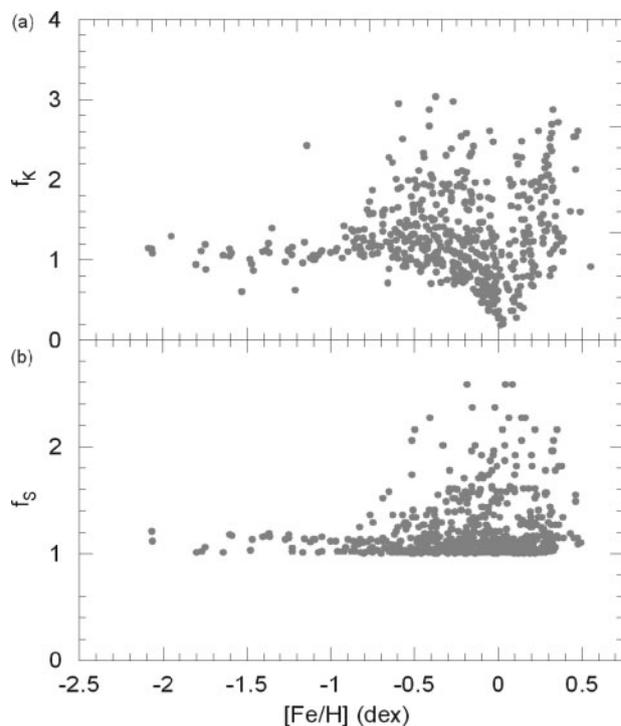
Figure 7 Guillotine factors versus metallicity for (a) metallicity-dependent guillotine factors (f_K) and (b) guillotine factors free of metallicity given by Sandage (1969) (f_S).

Figure 8 Metallicity calibration based on (a) the metallicity-dependent guillotine factors and (b) the guillotine factors adopted from Sandage (1969). The dashed lines denote the $\pm 1\sigma$ prediction levels.

distribution of the points about the line of zero residual is almost homogeneous, resulting in a zero correlation coefficient, $R^2 = 0.00$.

In Figure 10, the residuals are calibrated to linear equations of the metallicities. The panels (a) and (b) correspond to the residuals estimated via metallicity-dependent guillotine factors f_K and those of the metal-free ones f_S. The inclinations of the lines are 0.10 and 0.20 for panels (a) and (b), respectively, favoring the f_K factors. Also, the correlation coefficients, $R^2 = 0.03$ and $R^2 = 0.11$, for panels (a) and (b) respectively, confirm our argument. That is, by a smaller correlation coefficient we infer a relatively homogeneous distribution for the residuals in panel (a).

It is interesting that there are small differences in statistics for the two sets of data which can be explained either by the UBV data or metallicities used. We should remember that the metallicities for the first set (75 stars) were estimated spectroscopically, whereas for the second set (469 stars) a photometric procedure was used.

Summary

We used the data of 11 authors appearing in the PASTEL catalogue (Soubiran et al. 2010) and estimated metallicity-dependent guillotine factors f_K which are used in an improved metallicity calibration. The metallicities taken from different authors were reduced to the metallicities of Valenti & Fischer (2005), so a homogeneous set of metallicities could be obtained. There are differences

of the calibration based on metallicity-dependent guillotine factors. There is a small correlation for the residuals in panel (b) in Figure 9, $R^2 = 0.25$, which corresponds to the guillotine factors f_S, whereas in panel (a), where the residuals were based on the guillotine factors f_K, the

Table 5. Comparison of the original metallicities taken from the literature with those evaluated by using two different calibrations (Equations 7 and 8). Hip No is the Hipparcos number; δ is the ultraviolet excess; f_K and f_S are the guillotine factors estimated in this work and adopted from Sandage (1969), respectively; $\delta_{0.6}(K)$ and $\delta_{0.6}(S)$ are ultraviolet excesses reduced by means of f_K and f_S, respectively; [Fe/H]$_{obs}$, [Fe/H]$_K$, and [Fe/H]$_S$ are original metallicities taken from the literature and metallicities evaluated via Equations 7 and 8, respectively; Δ[Fe/H]$_K$, and Δ[Fe/H]$_S$ are residuals for two calibrations, where K and S refer to the data evaluated by means of the guillotine factors estimated in this work and those adopted from Sandage (1969)

Hip No	δ	f_K	f_S	$(\delta_{0.6})_K$	$(\delta_{0.6})_S$	[Fe/H]$_{obs}$	[Fe/H]$_K$	[Fe/H]$_S$	Δ[Fe/H]$_K$	Δ[Fe/H]$_S$
1599	0.085	1.112	1.01	0.095	0.086	−0.26	−0.362	−0.325	0.102	0.065
3206	0.02	1.597	1.61	0.032	0.032	−0.06	−0.024	−0.066	−0.036	0.006
6702	0.021	0.976	1.14	0.021	0.024	0.16	0.025	−0.033	0.135	0.193
8102	0.086	1.397	1.14	0.120	0.098	−0.38	−0.528	−0.389	0.148	0.009
10140	0.207	1.093	1.01	0.226	0.209	−0.99	−1.429	−1.162	0.439	0.172
10306	0.077	0.808	1.17	0.062	0.090	−0.38	−0.171	−0.344	−0.209	−0.036
15330	0.077	1.042	1.02	0.080	0.078	−0.20	−0.271	−0.282	0.071	0.082
17147	0.137	1.113	1.05	0.152	0.144	−0.76	−0.768	−0.673	0.008	−0.087
19814	0.126	1.209	1.09	0.152	0.137	−0.70	−0.769	−0.631	0.069	−0.069
21272	0.025	1.727	1.23	0.044	0.031	−0.03	−0.078	−0.061	0.048	0.031
22263	−0.022	1.307	1	−0.028	−0.022	0.10	0.194	0.125	−0.094	−0.025
22596	0.087	1.112	1.01	0.096	0.087	−0.32	−0.370	−0.331	0.050	0.011
27913	0.027	1.163	1.01	0.031	0.027	−0.05	−0.019	−0.044	−0.031	−0.006
33495	0.121	1.135	1.14	0.138	0.138	−0.84	−0.655	−0.637	−0.185	−0.203
35377	0.107	1.055	1.02	0.113	0.109	−0.38	−0.477	−0.453	0.097	0.073
36818	0.151	1.119	1.01	0.168	0.152	−0.83	−0.901	−0.732	0.071	−0.098
37853	0.155	1.105	1.02	0.171	0.158	−0.78	−0.923	−0.773	0.143	−0.007
38541	0.251	1.002	1.01	0.251	0.253	−1.76	−1.692	−1.553	−0.068	−0.207
38625	0.153	1.035	1.15	0.159	0.176	−0.93	−0.819	−0.906	−0.111	−0.024
38908	0.095	1.152	1.02	0.109	0.097	−0.36	−0.455	−0.383	0.095	0.023
42438	0.073	1.115	1.01	0.082	0.074	−0.27	−0.282	−0.260	0.012	−0.010
43726	−0.006	1.466	1.06	−0.008	−0.006	0.07	0.133	0.076	−0.063	−0.006
50384	0.078	1.183	1.11	0.093	0.087	−0.38	−0.347	−0.328	−0.033	−0.052
51248	0.068	1.117	1	0.076	0.068	−0.23	−0.250	−0.231	0.020	0.001
53070	0.184	1.094	1.13	0.202	0.208	−1.38	−1.194	−1.159	−0.186	−0.221
54772	0.197	1.075	1.17	0.211	0.230	−1.15	−1.287	−1.344	0.137	0.194
56997	0.016	1.608	1.14	0.025	0.018	0.03	0.005	−0.009	0.025	0.039
59750	0.128	1.135	1.13	0.146	0.145	−0.82	−0.716	−0.682	−0.104	−0.138
60632	0.227	1.018	1.17	0.231	0.265	−1.68	−1.478	−1.666	−0.202	−0.014
62207	0.095	1.03	1.152	0.110	0.098	−0.30	−0.459	−0.392	0.159	0.092
63559	0.175	1.097	1.03	0.193	0.181	−0.93	−1.111	−0.940	0.181	0.010
64394	0.015	1.186	1.01	0.018	0.016	0.06	0.035	0.001	0.025	0.059
64426	0.121	1.123	1.08	0.136	0.131	−0.66	−0.644	−0.589	−0.016	−0.071
64924	0.002	1.629	1.1	0.004	0.002	−0.02	0.092	0.048	−0.112	−0.068
69972	−0.036	1.631	2.01	−0.059	−0.073	0.26	0.266	0.245	−0.006	0.015
70681	0.218	1.077	1	0.235	0.218	−1.45	−1.523	−1.243	0.073	−0.207
71681	−0.01	1.652	1.47	−0.017	−0.015	0.14	0.162	0.106	−0.022	0.034
71683	−0.031	1.435	1.04	−0.044	−0.032	0.22	0.234	0.154	−0.014	0.066
72998	0.136	1.143	1.14	0.155	0.155	−0.63	−0.793	−0.751	0.163	0.121
73005	0.093	1.495	1.27	0.139	0.118	−0.55	−0.665	−0.508	0.115	−0.042
75181	0.11	1.075	1.02	0.119	0.113	−0.48	−0.519	−0.476	0.039	−0.004
80837	0.119	1.125	1.06	0.133	0.126	−0.64	−0.624	−0.556	−0.016	−0.084
81800	0.037	1.315	1.05	0.048	0.039	−0.01	−0.100	−0.092	0.090	0.082
82636	0.105	1.046	1.03	0.110	0.108	−0.38	−0.456	−0.447	0.076	0.067
84905	0.085	1.169	1.02	0.099	0.087	−0.56	−0.389	−0.326	−0.171	−0.234
88745	0.121	1.123	1.08	0.136	0.131	−0.42	−0.644	−0.589	0.224	0.169
89554	0.211	1.05	1.14	0.222	0.241	−1.44	−1.387	−1.439	−0.053	−0.001
96258	0.018	0.966	1.13	0.018	0.021	−0.13	0.038	−0.018	−0.168	−0.112
96901	−0.001	1.454	1.04	−0.001	−0.001	0.08	0.108	0.059	−0.028	0.021
97063	−0.016	0.833	1.13	−0.013	−0.018	0.02	0.149	0.114	−0.129	−0.094
98020	0.208	1.091	1	0.227	0.208	−1.37	−1.443	−1.160	0.073	−0.210
99026	0.037	0.549	1.17	0.020	0.043	0.02	0.027	−0.112	−0.007	0.132
99461	0.11	1.327	1.41	0.146	0.155	−0.58	−0.717	−0.751	0.137	0.171
99889	0.05	0.642	1.19	0.032	0.059	−0.05	−0.023	−0.185	−0.027	0.135
100568	0.187	1.092	1.05	0.204	0.196	−1.22	−1.215	−1.060	−0.005	−0.160
100792	0.154	1.125	1.13	0.174	0.174	−0.99	−0.944	−0.892	−0.046	−0.098
102011	0.047	0.622	1.17	0.029	0.055	−0.03	−0.010	−0.165	−0.020	0.135
102029	−0.021	0.807	1.15	−0.017	−0.024	0.15	0.162	0.133	−0.012	0.017
102485	−0.003	0.886	1.17	−0.003	−0.004	−0.11	0.116	0.070	−0.226	−0.180

(Continued)

Table 5.   (Continued)

| Hip No	δ	f_K	f_S	$(\delta_{0.6})_K$	$(\delta_{0.6})_S$	[Fe/H]$_{obs}$	[Fe/H]$_K$	[Fe/H]$_S$	Δ[Fe/H]$_K$	Δ[Fe/H]$_S$
102531	−0.057	0.609	1.12	−0.035	−0.064	0.12	0.211	0.228	−0.091	−0.108
103269	0.237	1.04	1.01	0.246	0.239	−1.60	−1.638	−1.424	0.038	−0.176
103498	0.171	1.099	1.08	0.188	0.185	−0.99	−1.070	−0.971	0.080	−0.019
104659	0.194	1.087	1.09	0.211	0.212	−1.42	−1.286	−1.188	−0.134	−0.232
105184	0.027	1.322	1.02	0.035	0.027	−0.14	−0.038	−0.045	−0.102	−0.095
105864	0.019	0.968	1.15	0.018	0.022	0.08	0.035	−0.023	0.045	0.103
109646	0.121	1.123	1.08	0.136	0.131	−0.59	−0.644	−0.589	0.054	−0.001
110778	0.071	1.116	1.01	0.079	0.071	−0.13	−0.264	−0.246	0.134	0.116
110785	0.011	1.449	1.08	0.016	0.012	−0.04	0.044	0.014	−0.084	−0.054
110996	−0.032	1.638	2.27	−0.053	−0.073	0.25	0.253	0.245	−0.003	0.005
113357	0.014	1.392	1.06	0.020	0.015	0.12	0.028	0.002	0.092	0.118
113896	0.035	1.148	1.01	0.041	0.036	−0.10	−0.064	−0.081	−0.036	−0.019
114081	−0.011	0.853	1.15	−0.010	−0.013	0.25	0.138	0.099	0.112	0.151
114096	0.037	1.315	1.05	0.048	0.039	0.09	−0.100	−0.092	0.190	0.182
114210	0.048	0.629	1.18	0.030	0.056	−0.17	−0.015	−0.173	−0.155	0.003
116824	0.02	0.41	1.19	0.008	0.023	0.09	0.076	−0.029	0.014	0.119
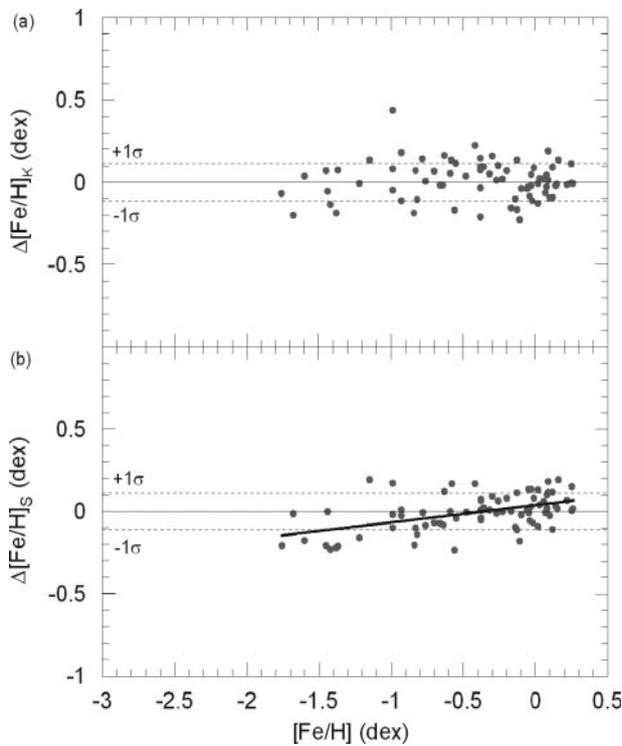
Figure 9 Metallicity residuals versus metallicity for 75 stars taken from Karaali et al. (2003), (a) for the calibration based on metallicity-dependent guillotine factors, and (b) for the calibration based on guillotine factors adopted from Sandage (1969). The dashed lines denote one standard deviation.

Figure 10 Metallicity residuals versus metallicity for 469 stars taken from Karataş & Schuster (2006), (a) for the calibration based on metallicity-dependent guillotine factors and (b) for the calibration based on guillotine factors adopted from Sandage (1969). The dashed lines denote one standard deviation. The inclination of the calibration line in the upper panel is less than the one in the lower panel, favoring the metallicity calibration based on metallicity-dependent guillotine factors.

between the new guillotine factors f_K and the factors f_S adopted from Sandage (1969).

We derived metallicity calibrations for two sets of guillotine factors using the same procedure and applied them to two different sets of data. The data of the first set were taken from Karaali et al. (2003), whereas those of the second set are from Karataş & Schuster (2006). For the first set, the mean deviations of the residuals for two calibrations are different. The agreement is only for
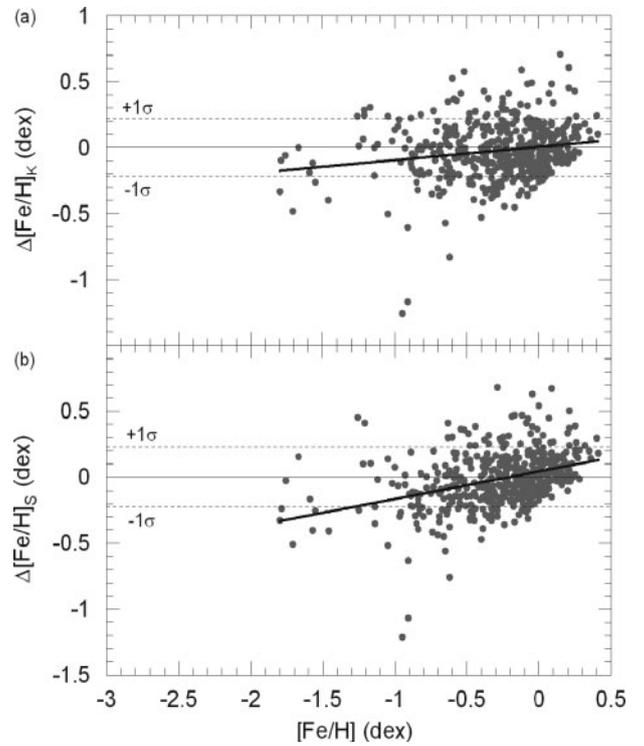
the metallicity interval $-1 <$ [Fe/H] ≤ -0.5 dex, whereas for the metallicity intervals $-1.76 <$ [Fe/H] ≤ -1, $-0.5 <$ [Fe/H] ≤ 0, and $0 <$ [Fe/H] $\leq +0.4$ dex, the mean deviations corresponding to the metallicity dependent guillotine factors f_K are much smaller than those estimated via the guillotine factors adopted from Sandage (1969), f_S. Also, the metallicity residuals for the total metallicity interval,

Table 6. Statistics for two metallicity calibrations based on new guillotine factors and the ones adopted from Sandage (1969), for two samples: (a) for 75 stars taken from Karaali et al. (2003) and (b) for 469 stars taken from Karataş & Schuster (2006)

	Mean deviation $\langle d[Fe/H] \rangle$		Standard deviation (σ)	
	This paper	Sandage (1969)	This paper	Sandage (1969)
(a) [Fe/H](dex)				
$-1.76 < [Fe/H] \leq -1.0$	-0.033	-0.123	0.116	0.139
$-1.0 < [Fe/H] \leq -0.5$	0.045	-0.039	0.149	0.110
$-0.5 < [Fe/H] \leq 0.0$	0.004	0.016	0.114	0.080
$0.0 < [Fe/H] \leq 0.4$	0.009	0.054	0.081	0.084
(b) [Fe/H](dex)				
$-1.76 < [Fe/H] \leq -1.0$	-0.040	-0.029	0.251	0.423
$-1.0 < [Fe/H] \leq -0.5$	-0.062	-0.131	0.278	0.255
$-0.5 < [Fe/H] \leq 0.0$	-0.034	0.010	0.198	0.187
$0.0 < [Fe/H] \leq 0.4$	0.036	0.095	0.166	0.177

$-1.76 < [Fe/H] \leq +0.4$, confirm the advantage of the metallicity-dependent guillotine factors.

For the second set, there is an agreement between the mean deviations for the two calibrations only for the metallicity interval $-1.76 < [Fe/H] \leq -1$ dex. The mean deviation of the residuals estimated via f_S for the metallicity interval $-0.5 < [Fe/H] \leq 0$ dex is a bit smaller than the mean deviation of those estimated via f_K, whereas for the two metallicity intervals $-1 < [Fe/H] \leq -0.5$ and $0 < [Fe/H] \leq +0.4$ dex the mean deviations corresponding to f_K are much smaller than those of f_S. In Figure 10, the residuals estimated via f_K and f_S are calibrated to linear equations of the metallicities. However, the inclination of the line for Figure 10(a) (0.10) is less than the one for Figure 10(b) (0.20), indicating that the metallicities estimated by means of the calibration based on metallicity-dependent guillotine factors agree better with the original metallicities relative to the other set of estimated metallicities.

We showed that the metallicity-dependent guillotine factors provide more accurate metallicities than those estimated by using the guillotine factors in the literature. This work will be useful for astronomers who work with UBV photometry, which has the advantage of being able to be transformed to other systems.

Acknowledgments

References

Ak, S., Bilir, S., Karaali, S. & Buser, R., 2007a, AN, 328, 169
Ak, S., Bilir, S., Karaali, S., Buser, R. & Cabrera-Lavers, A., 2007b, NewA, 12, 605
Bahcall, J. N. & Soneira, R. M., 1980, ApJS, 44, 73
Buser, R. & Kurucz, R. L., 1978, A&A, 70, 555
Buser, R. & Kurucz, R. L., 1985, Calibration of fundamental stellar quantities; Proceedings of the Symposium, Como, Italy, May 24–29, 1984 (Dordrecht: D. Reidel Publishing Co.), 513
Buser, R. & Fenkart, R. P., 1990, A&A, 239, 243
Buser, R. & Kurucz, R. L., 1992, A&A, 264, 557
Cameron, L. M., 1985, A&A, 152, 250
Carney, B. W., 1979, ApJ, 233, 211
Cayrel de Strobel, G., Soubiran, C. & Ralite, N., 2001, A&A, 373, 159
Fuhrmann, K., 2008, MNRAS, 384, 173
Hauck, B., Nitschelm, C., Mermilliod, M. & Mermilliod, J.-C., 1990, A&AS, 85, 989
Karaali, S., Bilir, S., Karataş, Y. & Ak, S., 2003, PASA, 20, 165
Karataş, Y. & Schuster, W., 2006, MNRAS, 371, 1793
Lejeune, Th., Cuisinier, F. & Buser, R., 1997, A&AS, 125, 229
Luck, R. E. & Heiter, U., 2006, AJ, 131, 3069
Marshall, D. J., Robin, A. C., Reylé, C., Schultheis, M. & Picaud, S., 2006, A&A, 453, 635
Mishenina, T. V., Soubiran, C., Kovtyukh, V. V. & Korotin, S. A., 2004, A&A, 418, 551
Nissen, P. E., Primas, F., Asplund, M. & Lambert, D. L., 2002, A&A, 390, 235
Ramirez, I. & Melendez, J., 2005, ApJ, 626, 446
Roman, N. G., 1955, ApJS, 2, 195
Ryan, S. G. & Smith, I. M., 2003, MNRAS, 341, 199
Sandage, A. & Eggen, O. J., 1959, MNRAS, 119, 278
Sandage, A., 1969, ApJ, 158, 1115
Santos, N. C., Israelian, G. & Mayor, M., 2004, A&A, 415, 1153
Schlegel, D. J., Finkbeiner, D. P. & Davis, M., 1998, ApJ, 500, 525
Schwarzschild, M., Searle, L. & Howard, R., 1955, ApJ, 122, 353
Soubiran, C., Le Campion, J.-F., Cayrel de Strobel, G. & Caillo, A., 2010, A&A, 515, A111
Sousa, S. G., Santos, N. C., Mayor, M., Udry, S., Casagrande, L., Israelian, G., Pepe, F., Queloz, D. & Monteiro, M. J. P. F. G., 2008, A&A, 487, 373
Spite, M., Francois, P., Nissen, P. E. & Spite, F., 1996, A&A, 307, 172
Strömgren, B., 1966, ARA&A, 4, 433
Tomkin, J. & Lambert, D. L., 1999, ApJ, 523, 234
Trefzger, Ch. F., Pel, J. W. & Gabi, S., 1995, A&A, 304, 381
Valenti, J. A. & Fischer, D. A., 2005, ApJS, 159, 141
van Leeuwen, F., 2007, ASSL, 350
Vandenberg, D. A. & Bell, R. A., 1985, ApJS, 58, 561
Wallerstein, G. & Carlson, M., 1960, ApJ, 132, 276
Wallerstein, G., 1962, ApJS, 6, 407
Walraven, Th. & Walraven, J. H., 1960, Bull. Astron. Inst. Netherlands, 15, 67
Wildey, R. L., Burbidge, E. M., Sandage, A. R. & Burbidge, G. R., 1962, ApJ, 135, 94
Yaz, E. & Karaali, S., 2010, NewA, 15, 234